

Effect of Drying Treatment on the Physical and Mechanical Properties of Material Extrusion-Based 3D-Printed PETG Models

Chen Wang,^{a,b,*} Hanyi Huang,^a Xiaowen Wang,^a Yiboran Wang,^a and Yu Zhu^a

Two rolls of PETG filament (1[#] and 2[#] filament) from the same manufacturer were placed in a constant temperature and humidity test chamber for moisture absorption pre-treatment for 12 h. The 2[#] filament was dried in a special dryer for 8 h. The physical and mechanical properties of the printed samples of 1[#] filament (without drying treatment) and 2[#] filament (with drying treatment) were compared. The R_a and R_z values of the samples printed on 2[#] filament were lower than those of the samples printed on 1[#] filament, and the samples printed on 2[#] filament were less rough. The light transmission of the samples printed on 2[#] filament was higher than that of the samples printed on 1[#] filament, and the light transmission properties of the samples printed on 2[#] filament were better. The tensile strength and elastic modulus of the samples printed on 2[#] filament were higher than those of the samples printed on 1[#] filament, and the mechanical properties of the samples printed on 2[#] filament were better. Therefore, the drying treatment improved the physical and mechanical properties of ME-3DP models, and this method has high application value.

DOI: 10.15376/biores.20.3.7000-7009

Keywords: Drying treatment; ME-3DP; PETG models; Physical and mechanical properties

Contact information: a: College of Furnishings and Industrial Design, Nanjing Forestry University, Nanjing 210037, China; b: Jiangsu Co-Innovation Center of Efficient Processing and Utilization of Forest Resources, Jiangsu, China; *Corresponding author: 996869559@qq.com

INTRODUCTION

Material extrusion-based 3D printing (ME-3DP) is one of the most popular 3D printing processes, featuring a simple moulding principle, low material cost, and high printing efficiency (Yang *et al.* 2022). ME-3DP technology uses layer-by-layer stacking to generate product prototypes. The physical and mechanical properties of ME-3DP models mainly include surface roughness, light transmission, tensile strength and elastic modulus. These properties are essential to ensure the quality and reliability of ME-3DP models (Feng *et al.* 2022).

Polyethylene terephthalate-1, 4-cyclohexanedimethanol ester (PETG) is a transparent plastic and a new type of ME-3DP filament with good thermoforming and chemical-resistant properties; it is economical and environmentally friendly, and it has a broad application prospect in the field of 3D printing (Chen *et al.* 2022). PETG is the product of the polycondensation of three monomers, terephthalic acid (PTA), bio-based ethylene glycol (BIOMEG), and 1, 4-cyclohexanedimethanol (CHDM), by ester exchange. Of these, BIOMEG, which is converted from sugar or other bio-based products from non-food resources, is a highly hydrophilic monomer that is prone to moisture absorption and

deterioration (Li *et al.* 2022). This also causes PETG filament to have strong moisture absorption and a high moisture content in its equilibrium state (generally between 0.1% and 0.4%), which affects the physical and mechanical properties of the ME-3DP models (Huang *et al.* 2022).

There is a growing research focus on the effect of moisture and water on the physical and mechanical properties of ME-3DP models. Zaldivar *et al.* (2018) investigated the moisture absorption characteristics of the ULTEM® 9085 filament and how the uptake concentration affected the quality of material extrusion manufactured 3D parts. The investigation emphasized the impact of humidity on the mechanical properties, roughness, and other metrics of ULTEM® 9085 filaments, as well as the need for awareness of the moisture sensitivities of ULTEM® 9085 when manufacturing high-quality material extrusion processed structures. Ghabezi *et al.* (2024) investigated the performance of continuous fibre-reinforced 3D-printed components in salt water medium at room temperature. An aging process was conducted to characterize the long-term effect of salt water on the mechanical behaviour of fibre-reinforced 3D-printed samples, and the mechanical tests revealed the degradation and loss in mechanical properties of the printed samples after aging in salt water. Adedotun *et al.* (2022) explored the effects of moisture and temperature on the mechanical properties of commonly used 3D printing polymers, such as polyamide (PA) and polylactic acid (PLA), during prolonged exposure to humidity and heat. The results show that for both PA and PLA filaments, there is a direct relationship between moisture absorption and the degradation of bending properties of 3D-printed models.

To reduce the moisture content of PETG filament and improve the physical and mechanical properties of ME-3DP models, drying treatment of PETG filament before 3D printing is an efficient and convenient method (Ding *et al.* 2022). However, the existing studies have provided less experimental analysis of the effect of drying PETG filament, especially from the perspective of physical and mechanical properties, which are the main indexes to reflect the printing quality of ME-3DP models (Li *et al.* 2023). Therefore, in this paper, the effects of drying treatment on the surface roughness, light transmission, tensile strength, and elastic modulus of ME-3DP models were investigated through comparative experiments to provide a reference for the effective improvement of the physical and mechanical properties of ME-3DP models (Wang *et al.* 2022). In addition, with the continuous development of ME-3DP technology, cellulose and its derivatives have been gradually applied to the preparation of ME-3DP materials and the improvement of the performance of printed products (Qi *et al.* 2023). Future research goals of this work are to analyse the physical and mechanical properties of the cellulose-based ME-3DP models and to improve the physical and mechanical properties of the cellulose-based ME-3DP models by optimizing the drying treatment (Deng *et al.* 2023).

EXPERIMENTAL

Materials

The PETG filament (Transparent, 1.75 mm diameter, Miracle 3D, Suzhou, China) with a density of 1.29 g/cm³ and a melting point of 180 °C was used for additive manufacturing by ME-3DP technology (Han *et al.* 2022). Two rolls of PETG filament from the same manufacturer were selected and numbered 1[#] and 2[#] respectively, of which the 2[#] filament was dried and the 1[#] filament was used as a reference group of material without drying.

Moisture Absorption Pre-treatment

To prevent moisture absorption and deterioration, ME-3DP filament is usually vacuum-packed in sealed bags when it is dispatched from the factory (Yu *et al.* 2024). After removing the sealed bags, two rolls of PETG filament (1[#] and 2[#] filament) were weighed by an electronic balance (BSA822, Sartorius, Gottingen, Germany), and the weights of the two rolls were 202.06 g and 202.22 g. Then, the two rolls were placed in a constant temperature and humidity test chamber for 12 h to simulate the process of moisture absorption of PETG filament in a high temperature and high humidity environment (30 °C and 90% humidity) (as shown in Fig. 1). After 12 h, the two rolls were removed from the constant temperature and humidity test chamber and weighed, and the weights of the two rolls were 202.75 g and 202.92 g, which indicated that the two rolls had gained 0.69 g and 0.70 g of weight by absorbing moisture, and the moisture content of the two rolls was 0.34% and 0.35%, respectively.

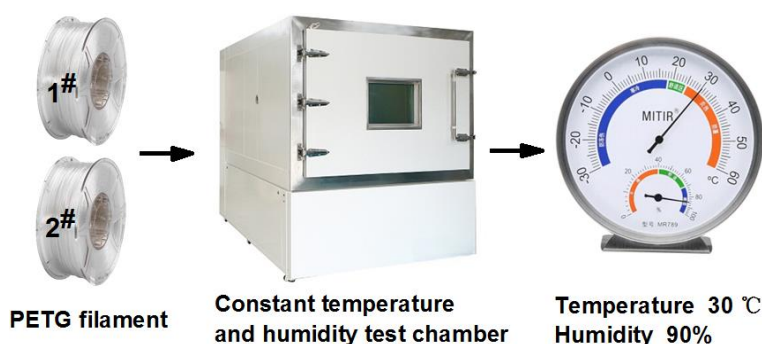


Fig. 1. Moisture absorption pre-treatment

Drying Treatment

Using ME-3DP filament special dryer to dry 2[#] filament after moisture absorption pre-treatment, drying temperature selection of 70 °C, drying time cumulative total of 8 h, every 1 h to remove the filament for weighing (weighing time is not counted in the drying time), drying treatment experiment are shown in Fig. 2.

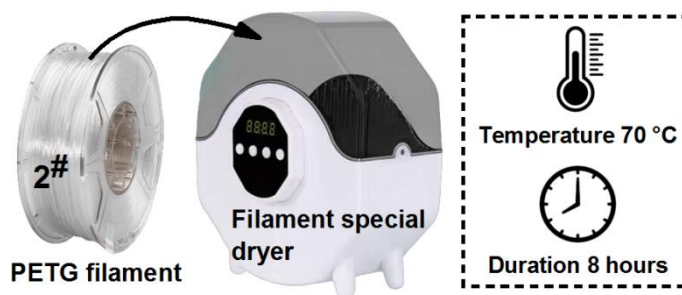


Fig. 2. Drying treatment

Sample Preparation

The 3D models of sample A, sample B and sample C were designed by SolidWorks software (shown in Fig. 3), and sample A, sample B and sample C were printed using a 3D printer (0.4 mm nozzle diameter, Anycubic, Shenzhen, China) with 1[#] and 2[#] filament, respectively. Among them, sample A was used to analyse the effect of the drying treatment on the surface roughness properties, sample B was used to analyse the effect of the drying

treatment on the light transmission properties, and sample C was used to analyse the effect of the drying treatment on the mechanical properties. The 3D printing process parameters were the same for all groups of specimens and are shown in Table 1.

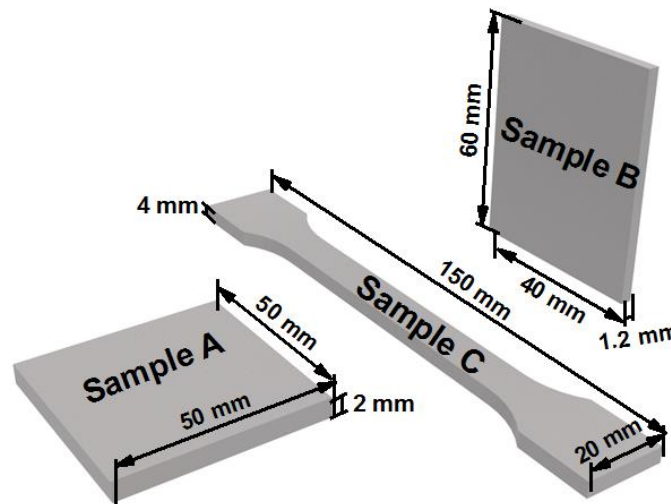


Fig. 3. 3D models of sample A, sample B and sample C

Table 1. 3D printing Process Parameters

Process Parameters	Settings
Printing layer height	0.2 mm
Build plate temperature	60 °C
Printing speed	50 mm/s
Nozzle temperature	200 °C
Infill percentage	100%
Infill pattern	Grids

Physical and Mechanical Properties Tests

The surface roughness of sample A was tested using a roughness tester (JB-4C, Taiming, Shanghai, China) with reference to the ISO 4287 (1997) standard. According to the experimental method specified in the standard, one measuring point was taken on the surface of sample A, and the measuring point was located in the centre of the top square. The arithmetic mean difference of the contour (R_a) and the maximum height (R_z) were selected as the surface roughness evaluation indexes. R_a is the arithmetic mean value of the absolute value of the distance from each point to the centre line of the contour on the measured contour within a certain sampling length, whereas R_z is the sum of the maximum contour peak height and the maximum contour valley depth on the measured contour within a certain sampling length.

The light transmission of sample B was tested using a UV spectrophotometer (U-3900, Hitachi, Tokyo, Japan) with reference to the ISO 26723-2020 standard. According to the experimental method specified in the standard, one measuring point was taken on the surface of sample B, and the measuring point was located in the centre of the side rectangle.

The mechanical properties of sample C (3 samples in each group) were tested using a universal mechanical testing machine (AG-X, Shimadzu, Kyoto, Japan) with reference to the ISO 527.2 (2012) standard. In the test, by applying a constant tensile speed (1

mm/min), the tests were carried out in a quasi-static loading condition at room temperature of 20 °C. By analysing the stress-strain relationship of specimen C during the tensile process, the property indexes such as tensile strength and elastic modulus of the specimen can be evaluated. Among them, tensile strength is the maximum value of stress in the specimen during tensile process, and elastic modulus is the ratio of stress and strain in the elastic deformation stage (Wang *et al.* 2023).

The microscopic features of PETG models were observed using an industrial flush-focus microscope (CL-MA-50M, Colomer, Guangzhou, China).

RESULTS AND DISCUSSION

Result of Drying Treatment

The ME-3DP filament dryer was used to dry 2[#] filament after moisture absorption pre-treatment, and the weight data obtained from the drying treatment experiments were plotted in Fig. 4. As shown in Fig. 4, the weight of the 2[#] filament gradually decreased with the increase of the cumulative drying time, which indicated that the moisture in the filament had been effectively dried. When the cumulative drying time was 8 h, the weight of filament was stable at 202.22 g, which was in the equilibrium state of moisture absorption.

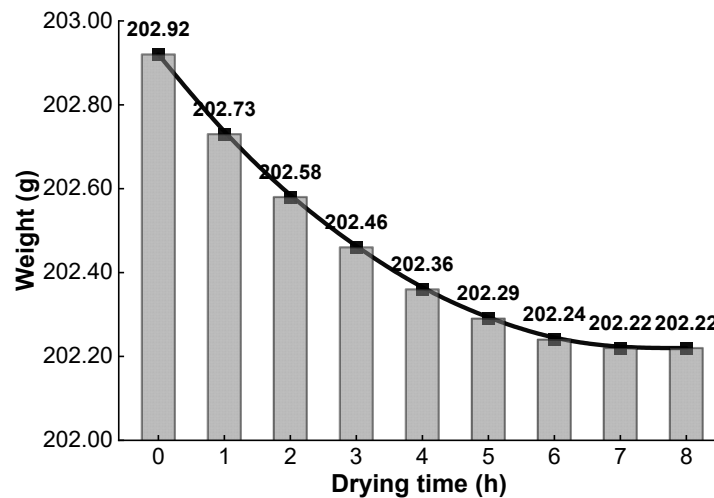


Fig. 4. 2[#] filament weight-drying time curve

Effect of Drying Treatment on Surface Roughness of PETG Models

Comparing the surface roughness of sample A printed on 1[#] filament and 2[#] filament, the results are shown in Figs. 5 and 6. As shown in Fig. 5, the R_a and R_z values of the samples printed on 2[#] filament were 48.03% and 67.26% lower than those of the samples printed on 1[#] filament, and the surface roughness of the samples printed on 2[#] filament was reduced. This is because the 1[#] filament was not dried. The moisture in the filament was evaporated by heat in the printer nozzle, which affected the smoothness of the extrusion process, resulting in uneven diameter of the molten filament extruded from the nozzle (Hu *et al.* 2021). When the molten filament having an uneven diameter was subjected to cooling and solidification, the vertical direction of the cross-section exhibited obvious undulation fluctuations (as shown in the surface contour curve a in Fig. 6), so the R_a and R_z values of the samples were larger. While 2[#] filament was dried, the moisture in

the filament was evaporated. As a result, the diameter of the molten filament extruded from the nozzle is more uniform, and after cooling and solidification, the fluctuations in the vertical direction of the cross-section are smaller (as shown in the surface contour curve b in Fig. 6), and thus the R_a and R_z values of the samples were smaller (Mo *et al.* 2022).

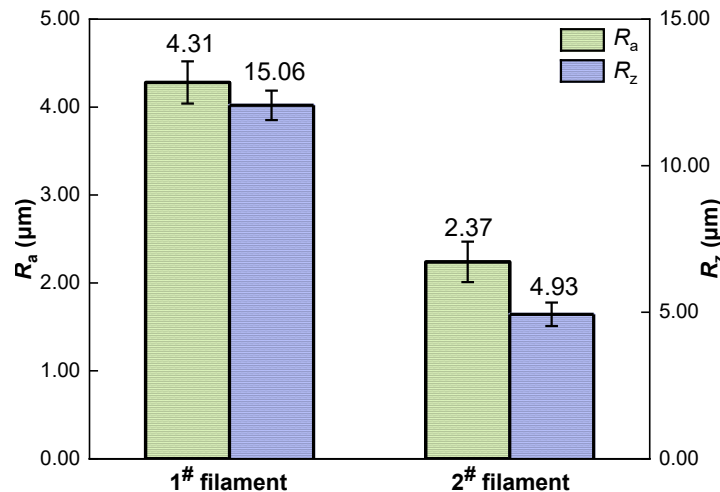


Fig. 5. Effect of drying treatment on surface roughness of PETG models

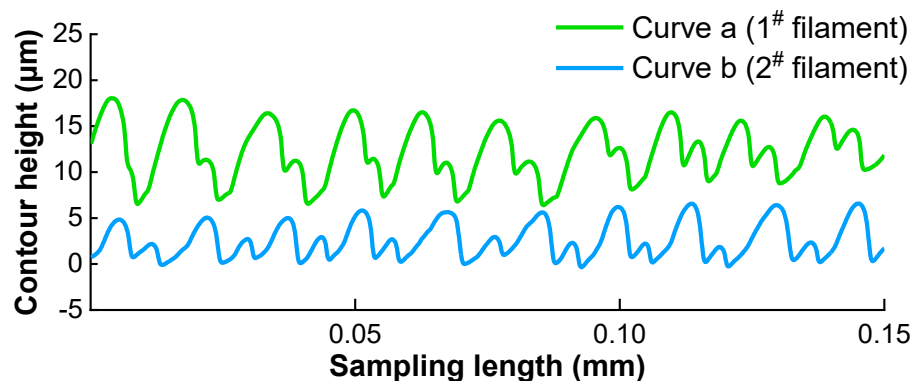


Fig. 6. Surface contour curve

Effect of Drying Treatment on Light Transmission Properties of PETG Models

Comparing the light transmission of sample B printed on 1[#] filament and 2[#] filament, the results are shown in Fig. 7. As can be seen in Fig. 7, the light transmission of the samples printed on 2[#] filament was 8.63%, 9.84%, 11.18% and 10.86% higher than that of the samples printed on 1[#] filament at the wavelengths of 400, 500, 600, and 700 nm, respectively, and the light transmission properties of the samples printed on 2[#] filament were better. This is because when the 1[#] filament (without drying treatment) flowed through the printer nozzle, the moisture present in the surface of the filament was evaporated by the heat and discharged, while the moisture inside the filament was not able to be discharged after evaporation by heat, so it still remained in the interior of the filament, and after cooling and solidification, a number of bubble cavities had been formed (as shown in Fig. 8a), which influenced the structural homogeneity of the samples (Xia *et al.* 2024). When the incident light passed through the samples, the bubble cavities caused a change

in the propagation medium, resulting in refraction and scattering of light. This weakened the intensity of the transmitted light, reducing the samples' light transmission properties (Zhou and Xu 2022). In the case of the 2[#] filament, due to the drying treatment, the moisture in the filament had been evaporated, so almost no bubble cavity was formed inside the filament during the printing process (as shown in Fig. 8b). There was no refraction and scattering of light, and the light transmission properties of the samples were significantly improved (Liu *et al.* 2021).

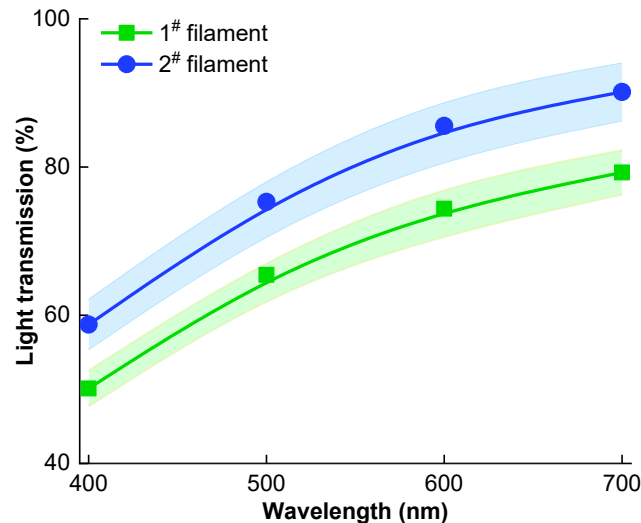


Fig. 7. Effect of drying treatment on light transmission properties of PETG models

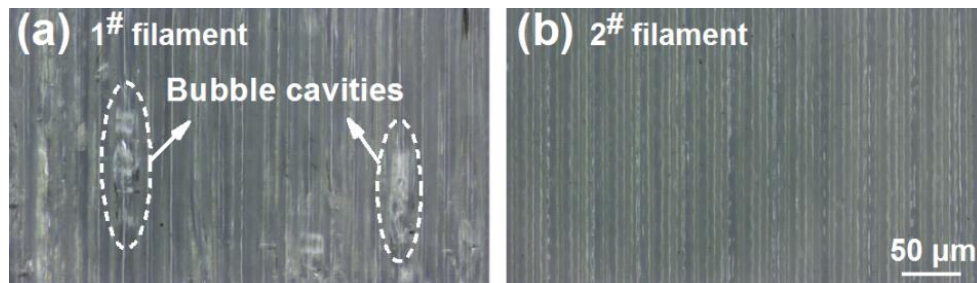


Fig. 8. Microscopic feature of bubble cavities

Effect of Drying Treatment on Mechanical Properties of PETG Models

Comparing the mechanical properties of sample C printed on 1[#] and 2[#] filament, the results are shown in Fig. 9. The tensile strength and elastic modulus of the samples printed on 2[#] filament were 18.1% and 17.0% higher than those of the samples printed on 1[#] filament, and the mechanical properties of the samples printed on 2[#] filament were better. This is because during the printing process of 1[#] filament (without drying treatment), due to the uneven diameter of the extruded molten filament, gaps were formed at the adhesive interface of adjacent layers of filament (as shown in Fig. 10a). Such structural defects are prone to cause stress concentration when the samples are subjected to load, leading to the degradation of the mechanical properties of the samples (Yu *et al.* 2023). As for the 2[#] filament, due to the drying treatment, the moisture in the filament was evaporated and discharged, and the gap defects are significantly reduced (as shown in Fig. 10b), and the mechanical properties of the samples are significantly improved (Hu *et al.* 2024).

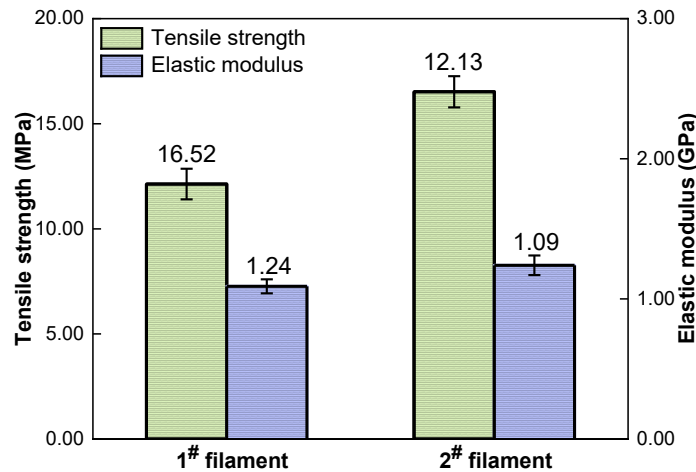


Fig. 9. Effect of drying treatment on mechanical properties of PETG models

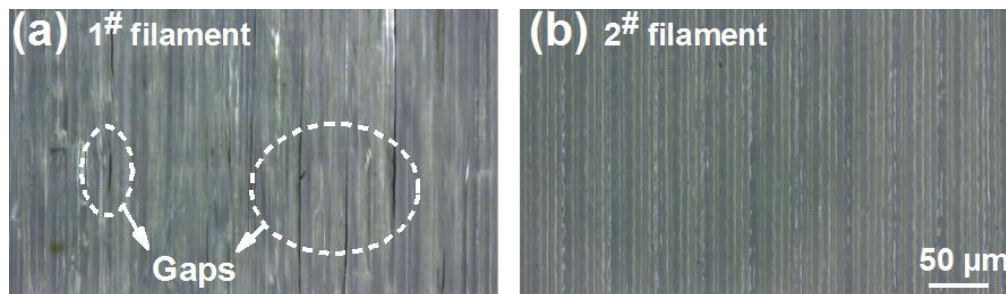


Fig. 10. Microscopic feature of gaps

CONCLUSIONS

The goal of this work was to demonstrate whether reduction of the moisture content of PETG filament would improve the physical and mechanical properties of ME-3DP models. Three sets of experiments were carried out to compare the surface roughness, light transmission, tensile strength, and elastic modulus of the printed samples of 1[#] filament (without drying treatment) and 2[#] filament (with drying treatment), respectively. The experimental results showed that the R_a and R_z values of the samples printed on 2[#] filament were lower than those of the samples printed on 1[#] filament, and the surface roughness of the samples printed on 2[#] filament was reduced. The light transmission of the samples printed on 2[#] filament is higher than that of the samples printed on 1[#] filament, and the light transmission properties of the samples printed on 2[#] filament was better, and the tensile strength and elastic modulus of the samples printed on 2[#] filament were higher than those of the samples printed on 1[#] filament. The mechanical properties of the samples printed on 2[#] filament were better. In summary, it was found that the drying treatment effectively improved the physical and mechanical properties of ME-3DP models.

Future research goals of this work are to analyse the physical and mechanical properties of the cellulose-based ME-3DP models and to improve the physical and mechanical properties of the cellulose-based ME-3DP models by optimising the drying treatment.

REFERENCES CITED

- Adedotun, D. B., Vinamra, A., Maria, L. A., and Asha-Dee, N. C. (2022). "Moisture-induced changes in the mechanical behavior of 3D printed polymers," *Composites Part C: Open Access*, 2022(7), article 100243. DOI: 10.1016/j.jcomc.2022.100243
- Chen, B.-R., Yu, X.-J., and Hu, W.-G. (2022). "Experimental and numerical studies on the cantilevered leg joint and its reinforced version commonly used in modern wood furniture," *BioResources* 17(3), 3952-3964. DOI: 10.15376/biores.17.3.3952-3964
- Deng, J.-Z., Huang, N., and Yan, X.-X. (2023). "Effect of composite addition of antibacterial/photochromic/self-repairing microcapsules on the performance of coatings for medium-density fiberboard," *Coatings* 13(11), article 1880. DOI: 10.3390/coatings13111880
- Ding, T.-T., Yan, X.-X., and Zhao, W.-T. (2022). "Effect of urea-formaldehyde resin-coated colour-change powder microcapsules on performance of waterborne coatings for wood surfaces," *Coatings* 12(9), article 1289. DOI: 10.3390/coatings12091289
- Feng, X.-H., Yang, Z.-Z., Wang, S.-Q., and Wu, Z.-H. (2022). "The reinforcing effect of lignin-containing cellulose nanofibrils in the methacrylate composites produced by stereolithography," *Polymer Engineering and Science* 2022(9), 2968-2976. DOI: 10.1002/pen.26077
- Ghabezi, P., Flanagan, T., Walls, M., and Harrison, N. M. (2024). "Degradation characteristics of 3D printed continuous fibre-reinforced PA6/chopped fibre composites in simulated saltwater," *Progress in Additive Manufacturing*, 10(1), 1-14. DOI: 10.1007/s40964-024-00654-5
- Han, Y., Yan, X.-X., and Zhao, W.-T. (2022). "Effect of thermochromic and photochromic microcapsules on the surface coating properties for metal substrates," *Coatings* 12(11), article 1642. DOI: 10.3390/coatings12111642
- Hu, W.-G., Li, S., and Liu, Y. (2021). "Vibrational characteristics of four wood species commonly used in wood products," *BioResources* 16(4), 7101-7111. DOI: 10.15376/biores.16.4.7101-7111
- Hu, W.-G., Zhao, Y., Xu, W., and Liu, Y.-Q. (2024). "The influences of selected factors on bending moment capacity of case furniture joints," *Applied Sciences* 14(21), article 10044. DOI: 10.3390/app142110044
- Huang, N., Yan, X.-X., and Zhao, W.-T. (2022). "Influence of photochromic microcapsules on properties of waterborne coating on wood and metal substrates," *Coatings* 12(11), article 1750. DOI: 10.3390/coatings12121857
- Li, S., and Hu, W.-G. (2023). "Study on mechanical strength of cantilever handrail joints for chair," *BioResources* 18(1), 209-219. DOI: 10.15376/biores.18.1.209-219
- Li, W.-B., Yan, X.-X., and Zhao, W.-T. (2022). "Preparation of crystal violet lactone complex and its effect on discoloration of metal surface coating," *Polymers* 14(20), article 4443. DOI: 10.3390/polym14204443
- Liu, Q., Gu, Y., Xu, W., Lu, T., Li, W., and Fan, H. (2021). "Compressive properties of green velvet material used in mattress bedding," *Applied Sciences* 11(23), article 11159. DOI: 10.3390/app112311159
- Mo, X.-F., Zhang, X.-H., Fang, L., and Zhang, Y. (2022). "Research progress of wood-based panels made of thermoplastics as wood adhesives," *Polymers* 14(1), article 98. DOI: 10.3390/polym14010098
- Qi, Y.-Q., Sun, Y., Zhou, Z.-W., Huang, Y., Li, J.-X., and Liu, G.-Y. (2023). "Response surface optimization based on freeze-thaw cycle pretreatment of poplar wood dyeing

- effect,” *Wood Research* 68(2), 293-305. DOI: 10.37763/wr.1336-4561/68.2.293305
- Wang, L., Han, Y., and Yan, X.-X. (2022). “Effects of adding methods of fluorane microcapsules and shellac resin microcapsules on the preparation and properties of bifunctional waterborne coatings for basswood,” *Polymers* 14(18), article 3919. DOI: 10.3390/polym14183919
- Wang, Q., Feng, X.-H., and Liu, X.-Y. (2023). “Functionalization of nanocellulose using atom transfer radical polymerization and applications: A review,” *Cellulose* 30, 8495-8537. DOI: 10.1007/s10570-023-05403-5
- Xia, F., Wang, W., Zhang, J.-H., Yang, Y.-T., Wang, Q.-Y., and Liu, X.-Y. (2024). “Improving weed control through the synergy of waste wood-based panels pyrolysis liquid and rice husks: A sustainable strategy,” *BioResources* 19(4), 7606-7618. DOI: 10.15376/biores.19.4.7606-7618
- Yang, Z.-Z., Feng, X.-H., Xu, M., and Rodrigue, D. (2022). “Printability and properties of 3D printed poplar fiber/polylactic acid biocomposites,” *BioResources* 16(2), 2774-2788. DOI: 10.15376/biores.16.2.2774-2788
- Yu, S.-L., and Wu, Z.-H. (2024). “Research on the influence mechanism of short video communication effect of furniture brand: Based on ELM model and regression analysis,” *BioResources* 19(2), 3191-3207. DOI: 10.15376/biores.19.2.3191-3207
- Yu, S.-L., Zheng, Q., Chen, T.-Y., Zhang, H.-L., and Chen, X.-R. (2023). “Consumer personality traits vs. their preferences for the characteristics of wood furniture products,” *BioResources* 18(4), 7443-7459. DOI: 10.15376/biores.18.4.7443-7459
- Zaldivar, R. J., Mclouth, T. D., Ferrelli, G. L., Patel, D. N., Hopkins, A. R., and Witkin, D. (2018). “Effect of initial filament moisture content on the microstructure and mechanical performance of ULTEM® 9085 3D printed parts,” *Additive Manufacturing* 24, 457-466. DOI: 10.1016/j.addma.2018.10.022
- Zhou, J.-C., and Xu, W. (2022). “Toward interface optimization of transparent wood with wood color and texture by silane coupling agent,” *Journal of Materials Science* 57(10), 5825-5838. DOI: 10.1007/s10853-022-06974-7

Article submitted: April 29, 2025; Peer review completed: June 14, 2025; Revisions accepted: June 23, 2025; Published: July 3, 2025.
DOI: 10.15376/biores.20.3.7000-7009